Available online at www.sciencedirect.com
ScienceDirect
Journal of Molecular Catalysis A: Chemical 279 (2008) 20–26
JOURNAL OF MOLECULAR CATALYSIS A: CHEMICAL
www.elsevier.com/locate/molcata

Influence of crystallinity and carbon content on visible light photocatalysis of carbon doped titania thin films

Ming-Show Wong *, Shih-Wei Hsu, K. Koteswara Rao, Chinthala Praveen Kumar

Department of Materials Science and Engineering, National Dong Hwa University, Hualien-974, Taiwan, ROC

Received 4 August 2007; received in revised form 21 September 2007; accepted 21 September 2007
Available online 29 September 2007

Abstract

Visible light responsive carbon doped TiO_2 films were developed by ion-assisted electron-beam evaporation using rutile powder as source material and two different gases, CO_2 and CO in the ion source as dopant source. The influence of beam current on the carbon content and crystallinity of the films was systematically studied to understand their effect on photocatalytic activity. More carbon content was incorporated when ion beam current was raised and when CO_2 gas was utilized as the ion source and it also resulted in shifting the absorbance edge of TiO_2 towards higher wavelength region. The TiO_xC_y film of well-crystallized anatase phase with 1.25 at.% carbon dopant from CO_2 source exhibited the lowest contact-angle close to zero and the best photocatalytic activity in terms of the reduction of silver ions to metallic silver and the degradation of methylene-blue under visible-light illumination. Post annealing the films at a higher temperature (500 °C) also improved the overall photocatalytic activities. This work demonstrates clearly that the photocatalytic performance of the TiO_xC_y films under visible light correlates well with the anatase crystallinity and carbon dopant concentration.

Keywords: Titanium dioxide; Carbon-doped titania; Visible-light photocatalyst; Photodegradation; Superhydrophilicity

1. Introduction

TiO_2 has been identified as the most effective and useful photocatalyst exhibiting interesting photo-induced photocatalysis and hydrophilicity. But the available titanium oxides are poor absorbers of photons in the solar spectrum and only absorb the ultraviolet light, which constitutes only a small fraction (<5%) of the solar spectrum [1]. The efficient utilization of solar energy is one of the major goals of modern science and engineering that will have a great impact on technological applications [2–6]. Consequently any improvement of the photocatalytic efficiency of TiO_2 by shifting its optical response to the visible region will have a profound positive effect. A number of approaches have been used to modify the semiconducting-natured TiO_2 for its use in the visible light photocatalysis [7–16].

Impurity doping is one of the typical approaches to extend the spectral response of a wide band gap semiconductor to visible light. An initial approach of doping TiO_2 with transition metals has been investigated extensively [7]. However, the photocatalytic activity of metal doping is impaired by thermal instability [7] and an increase in carrier-recombination [8]. Recently, some researchers have reported TiO_2 doped with non-metallic atoms like nitrogen [9–11], carbon [12,13], sulphur [14], iodine [15] and co-doping with nitrogen and flouorine [16]. All show high photocatalytic activity under visible light owing to band gap narrowing.

Among the anion doped TiO_2 powders or thin films, carbon doping has been theoretically claimed to have a potential advantage over nitrogen doping [17]. A more substitutional carbon incorporation results in narrower bandgap and hence better photocatalytic performance compared to a similar amount of nitrogen doping. Substitutional carbon atoms introduce new states (C2p) close to the valence band edge of TiO_2 (i.e. O2p states). As a result of this the valence band edge shifts to higher energy compared with the reference TiO_2 and the band gap narrows. The energy shift of the valence band depends on the overlap of carbon states and O2p states. A higher doping concentration of carbon results in higher energy shift due to significant overlap of carbon and oxygen states and this leads to narrower band gap in the compound [17]. Moreover, our earlier results

* Corresponding author. Tel.: +886 3 8634206; fax: +886 3 8634200.
E-mail address: mswong@mail.ndhu.edu.tw (M.-S. Wong).

1381-1169/$ – see front matter © 2007 Elsevier B.V. All rights reserved.
doi:10.1016/j.molcata.2007.09.024

strongly suggest that the photocatalytic performance is preferential to its anatase crystallinity for pure titania and to both anatase crystallinity and dopant concentration for doped titania films [10,18–20].

Recently, carbon doped TiO_2 films have been prepared by radio frequency (RF) magnetron sputtering and the hydrophilicity characteristics are found to depend on the amount of carbon doped in TiO_2 [21]. The nature, crystallinity and amount of carbon incorporated depend on the preparation strategy adopted. In the present paper, we report the preparation of carbon doped TiO_2 films (TiO_xC_y) by ion-assisted electron-beam evaporation method using CO and CO_2 as the source gases and their photocatalytic activity dependence on the crystallinity (crystal phase and crystallite size) and carbon content of as deposited films. Improvement of crystallinity is attempted by post annealing the films at 500 °C and the corresponding enhancement of phocatalytic behavior is assessed.

2. Experimental procedure

The ion beam assisted electron-beam evaporation system was assembled by Branchy Vacuum Technology Co., Ltd. (Toayuan, Taiwan) using rutile TiO_2 (99.99%) as a source material. The details of the system were described elsewhere [18]. The ion beam source was made by Veeco Inc. and the diameter of this Kaufman-type ion source was 3 cm. The distance between the rotating substrate holder and the evaporation source was 550 mm. The chamber was evacuated using a mechanical pump (ALCATEL-2033SD) and a cryopump (CTI-Cryo-Torr8®). The base pressure was 6.65×10^{-4} Pa. The pure films were deposited in oxygen atmosphere (6.65×10^{-3} Pa), and for the carbon doped films the working pressure was set to 1.74×10^{-2} Pa with 7 sccm of CO or CO_2 flow in the ion gun. The substrates were sputter-etched with argon ions (Ar^+) for 5 min prior to the deposition to remove any residual pollutants on the surface. The substrate temperature was maintained at 300 °C by quartz lamp. In order to incorporate significant dopant in the films, the ion gun beam current was varied from 0 to 35 mA and beam voltage was maintained at 1000 V with commonwealth scientific ion beam supply (IBS) controller. The deposition rate was adjusted to 0.2 nm s^{-1} by quartz crystal monitor for all the films to deposit a thickness of 1.2 μm. The film deposited without ion beam current using either CO or CO_2 as source gas is essentially pure TiO_2 and is referred as T1 hereafter. The films obtained with beam currents 10, 20 and 35 mA using the source gases CO and CO_2 are entitled as T2, T3, T4 and T5, T6, T7, respectively. To improve the crystallinity, the films which were initially deposited at a substrate temperature of 300 °C are further post annealed at 500 °C for 8 h.

The crystallinity of the films was investigated with a Rigaku D/MAX-2500V 18 kW low angle X-ray diffractometer (XRD) operating with Cu Kα radiation (λ = 1.54178 Å) at 40 kV and 200 mA. The grain size was calculated from the XRD patterns according to Scherrer equation. Raman spectra for the films were recorded on RENISHAW 1000B spectrometer. The absorption spectra were obtained using Hitachi 3300H UV–visible spectrophotometer. The TiO_xC_y films were deposited on quartz in order to avoid the UV–vis absorption of the Si substrate in the range of 300–600 nm. The surface morphology and composition were characterized by scanning electron microscopy equipped with energy dispersive spectroscopy (SEM/EDS, Hitachi 3500H). Carbon content in the TiO_2 films was determined by electron probe micro analyzer (EPMA) using JXA-8800 (JEOL, Japan).

The photocatalytic activity under visible-light illumination was characterized by (i) the variation of surface hydrophilicity evaluated by the change of water contact angle on the surface of the films (ii) the reduction of Ag^+ ions in 0.1 M $AgNO_3$ to Ag metal, and (iii) the degradation of 5 ppm methylene blue (MB) aqueous solution (Riedel-de Haen). The visible light source was a fluorescent lamp (Hitachi-FML27EX-N) with the wavelength distribution around 400–700 nm, the maximum intensity at 550 nm and the light intensity on sample surface around 1.51 mW cm^{-2}. The photocatalytic activity was performed for both the as prepared and the post annealed (500 °C) films.

The variation of surface hydrophilicity was determined at ambient conditions (i.e. 298 K, RH: 58%) using a commercial contact angle meter (FACE, Kyowa Kaimenkagaku, Japan). For silver reduction, the carbon doped films (dimensions 3 mm × 3 mm) are immersed in 2 ml of $AgNO_3$ solution (0.1 M conc.) and illuminated with visible light source for 3 h, after which the films were cleaned with de-ion water and dried for SEM analysis. For photodegradation of MB, a 1 cm × 1 cm thin film was immersed in 6 ml solution of MB (conc. 5 ppm) in dark at room temperature. After irradiation the solution for a definite time with visible light, the conc. of MB was measured by following the absorbance at 664 nm wavelength of MB with UV–vis spectrometer.

3. Results and discussion

Fig. 1a and b show the XRD patterns of pure and carbon doped TiO_2 films before and after annealing. Prior to annealing, all films except T4, T6 and T7 exhibit pure anatase titania phase though the XRD peaks in carbon doped films are little broad, less intense and shifted to lower angle side as the beam current is increased from 10 to 35 mA. This is attributed to the ion bombardment and to the incorporation of carbon atoms in place of oxygen. As the beam current is increased the high energetic beam bombards the surface of depositing film and thereby induces atomic shuffling. Films become more defective as energetic ions from source gas insert themselves in and forcibly displace oxygen atoms of TiO_2 from equilibrium sites. These processes lead to a reduction of film crystallinity and is reflected in the form of broad and less intense peaks in the XRD pattern. Changes in the interplanar spacings and film orientations are also expected with increasing ion energy or flux due to the incorporation of carbon atoms or associated defects. The increased lattice constant with the energetic ion bombardment (increased beam current) results in the shift of XRD peaks for carbon doped films towards lower angle. In films T4, T6 and T7, small fraction of rutile phase was also observed. At the same time, composition analysis by EPMA indicates an increase in the carbon content with the increasing beam current. The incorporated carbon along

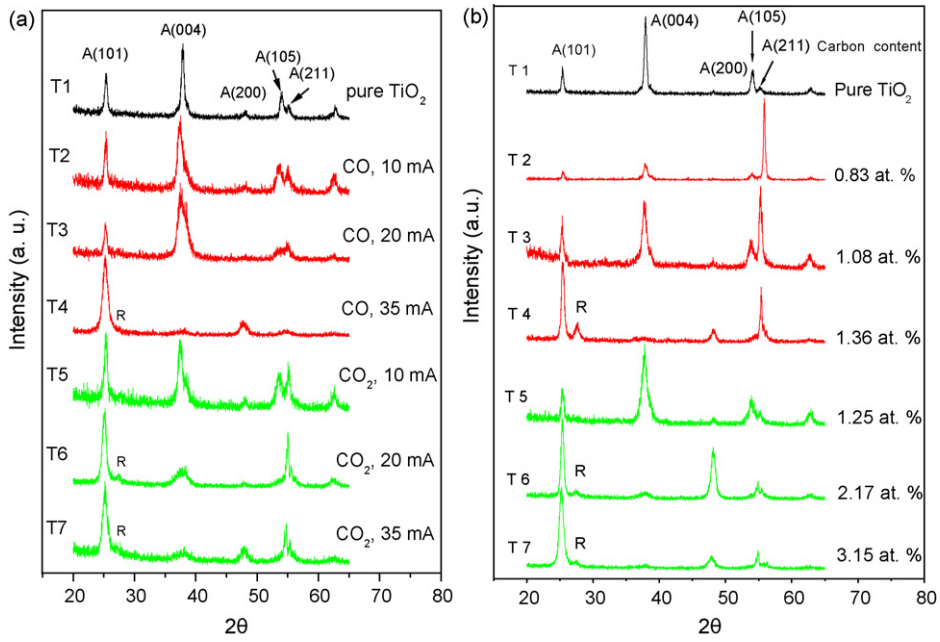

Fig. 1. XRD patterns of pure and carbon doped TiO_2 films obtained using CO and CO_2 as source gases at different beam currents (a) before annealing and (b) after annealing.

with high energetic beam decreases the crystallinity and therefore, the films deposited with a beam current of 10 mA are more crystalline compared to the films deposited with higher beam currents.

For the same beam current, the carbon content in the films deposited with CO_2 as source gas is always higher than that from CO. Scherrer's equation was applied to the most intense anatase peak ((1 0 1) or (0 0 4)) which provided a mean grain size in the range of ~15–20 nm. Calculations from the XRD peak positions also reveal that an anisotropic lattice expansion occurs with increased carbon content. The calculated lattice parameters 'a' and 'c' lie in the range 3.7870–3.8218 Å and 9.2977–9.6226 Å, respectively while the standard values from the XRD data base are, $a = 3.7852$ Å and $c = 9.5139$ Å (JCPDS card No. 21–1272).

The XRD patterns of films post annealed in air under normal humidity and atmospheric pressure are shown in Fig. 1b. The annealing affects grain growth in anatase (2 1 1) plane for the films T2, T3 and T4, while the sharpness of diffraction peaks (i.e. the FWHM of the peak) in general improved for all samples indicate increased crystallinity. But for T4, T6 and T7, the emergence of peaks corresponding to rutile phase (especially T4) and a (2 0 0) orientation preference of anatase phase is observed more prominently upon annealing. In an earlier report [22], carbon doped titania obtained by temperature-programmed carbonization (TPC) of anatase phase exhibits an inhibition towards rutile phase formation. In the present study, the continuation of rutile phase upon post annealing is due to the existence of small amount of rutile phase in the as deposited films of T4, T6 and T7. The formation of rutile TiO_2 in T4, T6 and T7 is probably due to the ion bombardment effects, since these samples were produced under higher ion flux. However, the crystallinity has been improved in the low carbon content samples (T1, T2, T3 and T5 with 0, 0.8, 1.1 and 1.25 at.% C, respectively) besides retaining the anatase phase.

The Raman spectra display a consistent result with that from XRD patterns and the films exhibit primarily a well-crystallized anatase structure as shown in Fig. 2a and b, before and after annealing, respectively. The anatase titania is characterized [23] by the obvious bands at 398, 518 and 640 cm^{-1} but the band around 518 cm^{-1} was overlapped with silicon substrate. Upon e-beam heating, TiO_2 source can be vaporized and may be decomposed into Ti, O, O_2 and TiO species, which proceed to rearrange on the substrate. However, the sample T1 is stoichiometrically TiO_2 only and not TiO_{2-x}. The Raman spectra of T1 clearly indicate the absence of any bands corresponding to lower oxides of Ti, for example Ti_2O_3 or TiO. But the small bands around 267 cm^{-1} observed for T2, T3 and T4 are due to the formation of Ti_2O_3 [24]. It is well known that rutile TiO_2 is a thermodynamically stable phase and generally forms at high temperatures (>800 °C) while anatase is a kinetically controlled crystal structure which can form at sufficiently low temperature (<500 °C). Hence, the films grown at 300 °C of substrate temperature would prefer to the formation of anatase phase (Fig. 2a). The intensity of anatase titania bands decreased with beam current, in films obtained from both source gases CO (T2, T3, T4) and CO_2 (T5, T6, T7), due to the ion bombardment and the carbon incorporation in the doped films. The ion bombardment and carbon incorporation decreases the crystallinity of films due to induced defects and therefore the Raman bands whose intensity depends on the crystallinity also gets decreased, correspondingly. However, the Raman spectra of post annealed films (Fig. 2b) show intense and sharp bands due to increased crystallinity (upon annealing out the defects) compared to the peaks in non-annealed films. But the peaks corresponding to rutile phase titania in T4, T6 and T7 are not distinctly visible as they

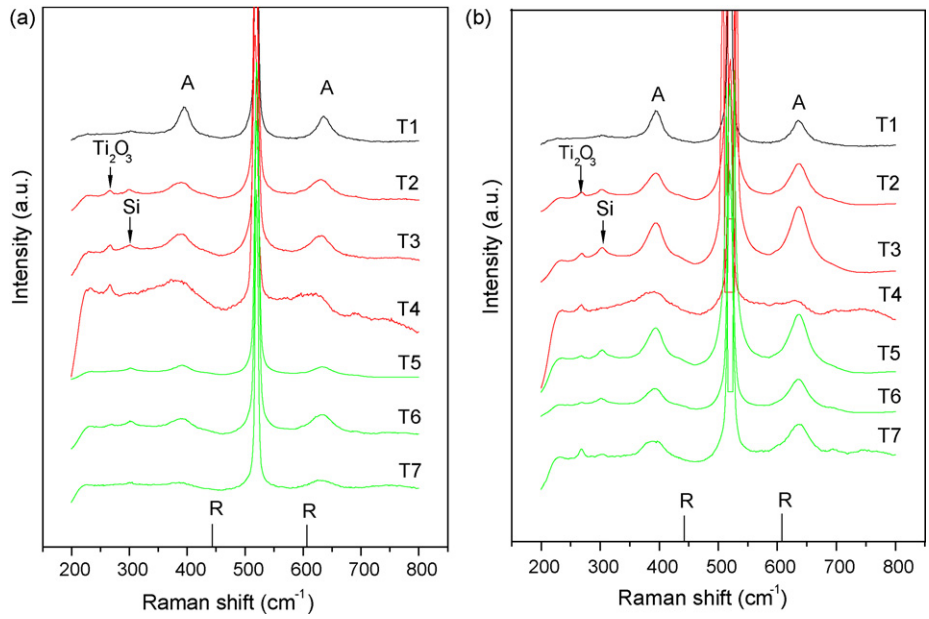

Fig. 2. Raman spectra of pure and carbon doped TiO_2 films (a) before annealing and (b) after annealing.

were submerged as shoulders in the 398 and 640 cm^{-1} peaks of anatase. The low concentration of rutile phase and the close proximity of peak position to anatase phase deter a clear observation of rutile phase in Raman spectra. Thus, these findings are consistent with the XRD results.

The deposition condition (such as, beam current, gas source) usually determines the composition and microstructure and therefore the properties. However, considering the variation of incorporated carbon (increasing carbon content) and anatase phase crystallinity, we feel that the films T1, T2, T3 and T5 would constitute a good combination for further study compared to other films which contain 1.35 at.% or more amount of carbon and also possessed a small amount of rutile phase in them. Though T5 is prepared with a different source gas compared to T1, T2 and T3, we consider it reasonable to choose crystal phase (anatase) as a primary step along with increasing carbon content, for grouping them together for further study. Here the selection of anatase phase for comparison is only a criterion based on the vast literature, in which anatase phase is proved to be a better photocatalyst compared to rutile or mixed phases.

Fig. 3 shows the UV–vis absorption spectra of undoped (T1) and carbon-doped (T2, T3 and T5) TiO_2 films before annealing. Carbon substitution causes a considerable shift in the absorbance edge of TiO_2 towards higher wavelength region. The pure TiO_2 film shows the absorption edge at ~380 nm and its absorption edge red-shifted gradually to ~410 nm in T2 and ~430 nm in T3 films. But the absorption edge of T5 is less than T3. The shift in the visible light region is largely due to inclusion of carbon into TiO_2 network to form Ti–C bonds. Similar optical spectra were obtained by Irie et al. [21] in the carbon doped titania films with the absorption shift mainly dependant on the carbon content. The UV–vis spectra of samples T4, T6 and T7 are taken but not shown for clarity, since they are all red shifted from the formation of rutile phase. But when the films were annealed, the UV–vis spectra (not presented here) did not show an appreciable red shift, instead showed a slight blue shift especially for T3, T4, T6 and T7. This result suggests the role of oxygen vacancies or defects induced by the high energy beam used for deposition. Before annealing, the defects form isolated localized bands in the energy gap and hence can lead to absorption of higher wavelengths. After annealing, however, the oxygen vacancies or defects are reduced and the absorption shifts to lower wavelengths again. So, the better absorption of film T3 in the visible region is apparently due to the relatively more defects formed by the higher flux of the high-energy beam used. The intensity of peak corresponding to Ti_2O_3 in the Raman spectra of T3 and T5 before and after annealing also corroborates this result. The little red-shift of the optical spectra of the carbon-doped titania (T2, T3 and T5) in Fig. 3 is mainly due to: (1) The contents of doped carbon in the titania films is relatively low, 1.25 at.% at the most, and (2) The films were grown at a

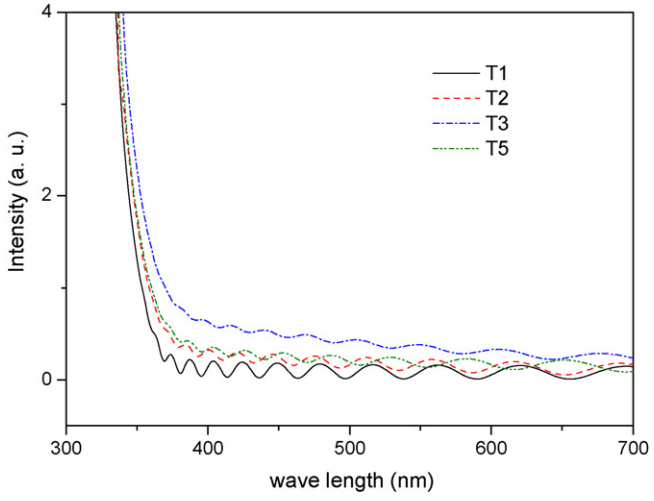

Fig. 3. UV–vis absorption spectra for T1, T2, T3 and T5 titania films before annealing.

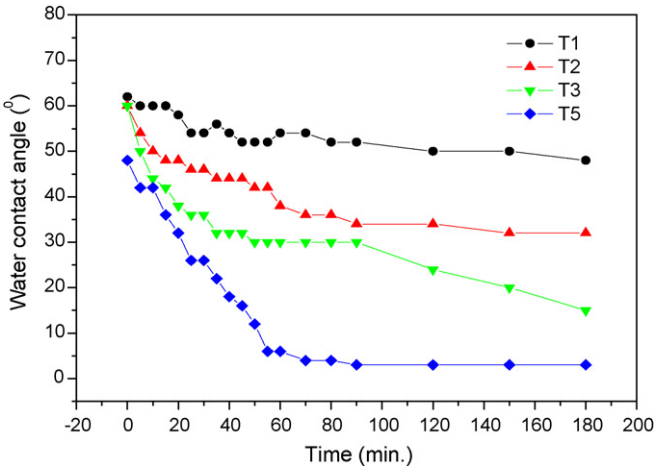

Fig. 4. Water contact angle variations following the visible light illumination time for T1, T2, T3 and T5 titania films before annealing.

substrate temperature of 300 °C, at which some of defects generated by ion bombardment could be annealed out. Therefore, the effects of the carbon incorporation and the creation of defects from ion bombardment are reflected in the absorption spectra of carbon doped titania films.

Water contact angle measurements were conducted to examine the visible-induced hydrophilicity of pure and carbon doped TiO_2 films. Fig. 4 shows the contact angle variation following the time of visible light illumination for T1, T2, T3 and T5 before annealing. The pure TiO_2 film (T1) shows the angle reduction from 62 to 48° after 90 min of visible light illumination. The T2 and T3 films display the angle reduction from 58 to 36° and 60 to 30°, respectively. However, the T5 film showed the highest reduction (48 to 3°) corresponding to the best hydrophilicity on the surface under visible light illumination. The hydrophilicity characteristics of carbon doped TiO_2 films studied earlier [21] showed a reduction of water contact angle from 20 to 13° even for the optimum carbon content of 1.1 mol% in the films. The large reduction of water contact angle in T5 indicates a better performance. The mechanism for the conversion from hydrophobic to hydrophilic under illumination was explained [25] by assuming that surface Ti^{4+} sites were reduced to the Ti^{3+} states via the photogenerated electrons, and oxygen vacancies were generated through the oxidation of the bridging O^{2-} species to oxygen via the photogenerated holes. Dissociated water gets adsorbed on the vacancy sites to create hydrophilic hydroxyl groups on the surface. The better performance of T5 compared to the films obtained by RF magnetron sputtering [21] could be partly due to the presence some Ti^{3+} sites along with oxygen vacancies and also due to the presence of a higher carbon content in T5. The carbon content in all films is obtained from EPMA as well as XPS. T5 showed a carbon content of 1.25 at.% and also anatase phase crystallinity even after post annealing treatment. As T1, T2 and T3 are also of anatase phase with high crystallinity after post annealing, the high carbon content in T5 in comparison to them is considered to be responsible for better photocatalytic performance. The XPS depth profiles (not shown here) of the films reveal that C–C bond exists on the film surface but diminishes with ion etching and finally gets replaced by Ti–C bond [20].

Fig. 5 shows the surface morphology (SEM images) of silver ion (Ag^+) reduction on the non-annealed (left side of panel) and annealed (right side of panel) films T1, T2, T3 and T5,

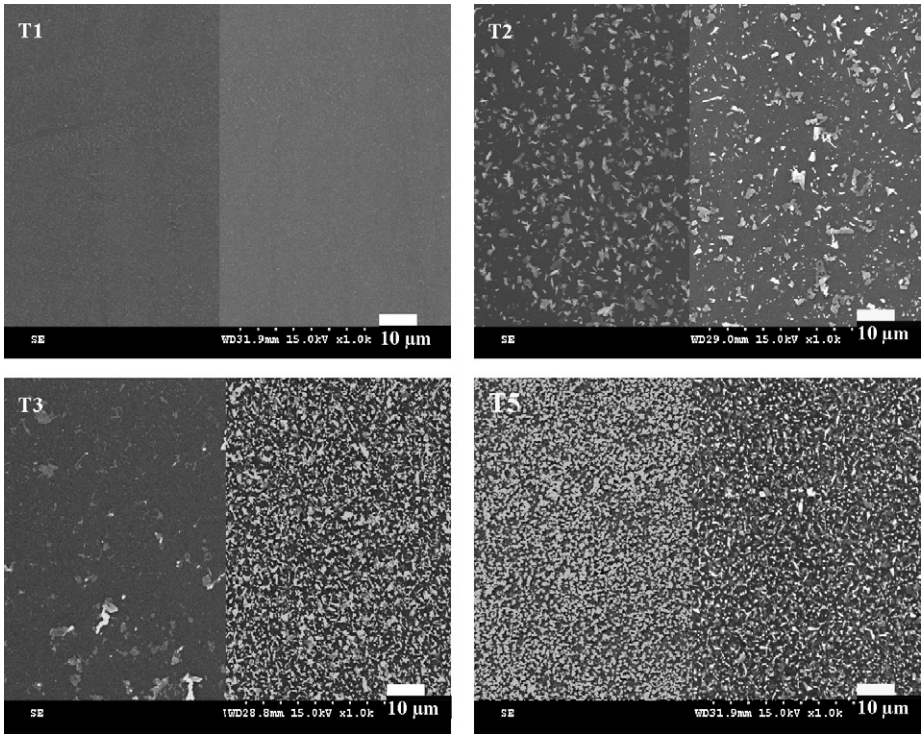

Fig. 5. SEM images of silver ion reduction for T1, T2, T3 and T5 titania films before (left) and after annealing (right).

Table 1
Beam current and carbon content dependant characteristics of photocatalytic properties before and after annealing the carbon doped titania films

Film	Carbon source gas	Beam current (mA)	Carbon content (at.%)	Annealing effect on photocatalytic properties			
				Rate constant (K, h^{-1})		Relative Silver (%)	
				Before	After	Before	After
T1	–	0	~0	0.042	0.042	0	0
T2	CO	10	0.8	0.084	0.140	2.9	2.6
T3	CO	20	1.1	0.069	0.161	1.0	9.8
T4	CO	35	1.36	0.052	0.083	0	0
T5	CO_2	10	1.25	0.108	0.170	7.7	10.6
T6	CO_2	20	2.2	0.082	0.091	1.2	1.2
T7	CO_2	35	3.2	0.059	0.062	0.1	0.5

respectively. Bulk silver particles are formed by the reduction of aqueous $AgNO_3$ solution on the surface of carbon doped TiO_2 films while no silver formation is shown for pure TiO_2 even after annealing. The relative amount of reduced silver quantified by EDS is presented in Table 1. In the non-annealed films, the amount of reduced silver follows the order T3 < T2 < T5 while in the annealed films the order is T2 < T3 < T5. The improved performance of T3 after annealing for photocatalytic reduction of Ag^+ is specifically due to the enhanced crystallinity upon annealing (Fig. 5). However, the film T5 showed the best performance due to more carbon content and perfect anatase crystallinity unlike T6 and T7 (for whom the SEM images are not shown but the data is presented in Table 1). The photocatalytic performance before and after annealing are compared in Fig. 6 which shows an overall increase of silver content in the annealed films of different carbon concentration.

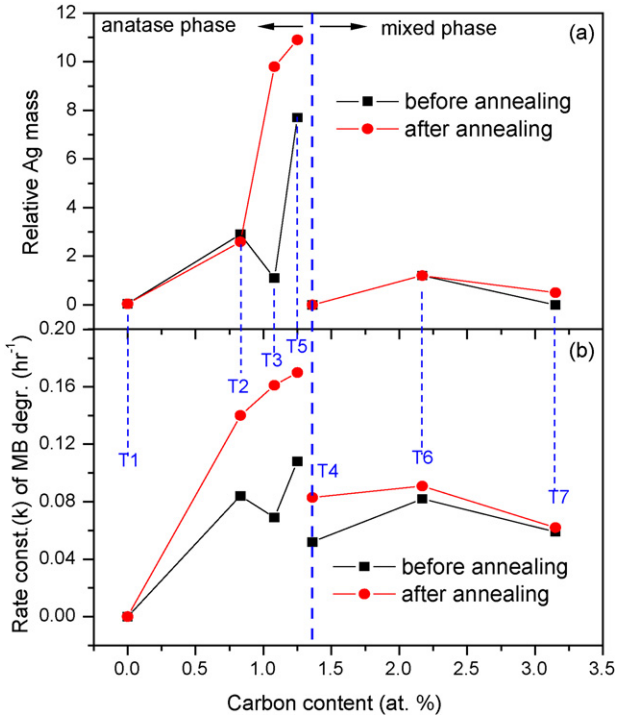

Fig. 6. Annealing effect on photocatalytic behavior of TiO_2 and TiO_xC_y films for (a) reduction of Ag^+ and (b) degradation of MB with different carbon content upon visible light illumination.

The visible light-induced photodegradation of MB for pure TiO_2 and carbon doped TiO_2 films was studied. The plot of the natural log of the MB concentrations versus irradiation time is a straight line. Thus, the kinetics of MB degradation suggested a first order mechanism, and the rate constants are presented in Table 1. The non-doped anatase film has a rate constant of 0.042 h^{-1} and the value does not change after the annealing, while the carbon-doped titania films all have higher rate constant. Among the carbon-doped titania films, those of pure anatase crystallinity (T2, T3 and T5) possess higher rate constant values which increasing with the carbon content in the films, while the films of mixed phases of rutile and anatase or amorphous phase have lower rate constants. After annealing, the rate constants for all the carbon-doped titania films become higher, but the films of pure anatase phase exhibit larger increment than those of mixed phases. The overall improvement of rate constants in annealed films as a function of carbon content is illustrated in Fig. 6. Analogous to superior hydrophilic performance, the film T5 (containing 1.25 at.% C) showed best photocatalytic activity with a rate constant of 0.108 h^{-1} before annealing which increased to 0.170 h^{-1} upon annealing. However, after annealing, a marked improvement in the rate constant is shown by T3, almost attaining that of film T5. This is reasonable, since T3 and T5 have very close amount of carbon dopant and about the same crystallinity after annealing.

The improvement of catalytic activity in the lower carbon content region (up to 1.25 at.% C) implies an optimum carbon content in carbon doped TiO_2 thin films by electron beam evaporation method. The crystallinity and carbon content are dependent on the beam current. This method of deposition with CO and CO_2 as source gases offered a means of controlling these crucial parameters for evaluating their photocatalytic performance. Annealing of films led to mixed anatase and rutile phase formation beyond the 1.25 at.% of carbon content (shown as thick dotted line in Fig. 6), i.e. in films T4, T6 and T7. The reason for the more incorporation of carbon in titania films using CO_2 gas can be attributed to the less bond dissociation energy of double bonded CO_2 than triple bonded CO. Moreover, the poisonous nature of CO makes it a less viable option compared to CO_2 gas.

Our prior studies and many other literatures have shown the photocatalytic properties of pure and nitrogen doped titania are proportional to composition and anatase crystallinity of the sam-

ples. Photocatalytic performance deteriorates a lot, if the phase is deviating from pure anatase to those consisting of amorphous, rutile or mixed phases. The results of this carbon-doped titania work again support the previous findings. The films T2, T3 and T5 are of anatase phase with varying crystallinity. After annealing, they possess about the same crystallinity but with increasing doped carbon content (T2 < T3 < T5) their photocatalytic properties also increase accordingly. On the other hand, the films T4, T6 and T7 before and after annealing are all of mixed phases, so their photocatalytic performance is rather poor.

The carbon species or states and defects in C-doped titania that induced a visible-light photocatalytic activity have still remained controversial. The incorporation of carbon atoms into titania inevitably influence the crystallinity and defect density in the films. The defects may include various kind of defects in the lattice, color centers (oxygen vacancies) and the doping of the lattice by C-species. These defects all contribute to the absorption of visible light and to the photocatalytic effect. For titania samples in either powder or film form, it is very hard to differentiate the type of defects and their corresponding photocatalytic effect. Our work demonstrates that the effect of carbon doping in titania lattice is evident through a series of annealed anatase films of varying carbon content but with comparable defect density and crystallinity.

4. Conclusion

This study demonstrates the effectiveness of using carbon monoxide (CO) and carbon dioxide (CO_2) gases for the preparation of carbon doped TiO_2 films by ion-assisted electron-beam evaporation. The beam current had a significant influence on the carbon content of the films and their crystallinity. At a beam current of 10 mA, the carbon doped TiO_2 film deposited using CO_2 gas is found to exhibit superior photocatalytic properties compared to other films. This is attributed to the optimum carbon incorporation with most favorable crystallinity in the film. An increase in titania crystallinity by annealing the films at 500 °C for 8 h gave favorable results in terms of photocatalytic performance. On the whole, the annealed carbon doped TiO_2 anatase film with the most doped carbon content of 1.25 at.% gave the best visible light photocatalytic activity for superhydrophilicity, degradation of MB and reduction of silver ions.

Acknowledgments

The authors are thankful for the financial support of National Science Council of Taiwan ROC under grant no. NSC 94-2216-E-259-002 and NSC 95-2120-M-259-001.

References

[1] S. Yin, Q.W. Zhang, F. Saito, T. Sato, Chem. Lett. 32 (2003) 358.
[2] A. Fujishima, K. Honda, Nature 238 (1972) 37.
[3] D.S. Ollis, H. Al-Ekabi, Photocatalytic purification and treatment of water and air, Elsevier Publications Ltd., Amsterdam, 1993.
[4] S.U.M. Khan, J. Akikusa, J. Phys. Chem. B 103 (1999) 7184.
[5] S. Licht, B. Wang, S. Mukerji, T. Soga, M. Umeno, H. Tributsch, J. Phys. Chem. B 104 (2000) 8920.
[6] R. Wang, K. Hashimoto, A. Fujishima, M. Chikuni, E. Kojima, A. Kitamura, M. Shimohigoshi, T. Watanabe, Nature 388 (1997) 431.
[7] W. Choi, A. Termin, M.R. Hoffman, J. Phys. Chem. 98 (1994) 13669.
[8] H. Yamashita, M. Honda, M. Harada, Y. Ichihashi, M. Anpo, T. Hirao, N. Itoh, N. Iwamoto, J. Phys. Chem. B 102 (1998) 10707.
[9] R. Asahi, T. Morikawa, T. Ohwaki, K. Aoki, Y. Taga, Science 293 (2001) 269.
[10] M.C. Yang, T.S. Yang, M.S. Wong, Thin Solid Films 469–470 (2004) 1.
[11] C. Burda, Y. Lou, X. Chen, A.C.S. Samia, J. Stout, J.L. Gole, Nano Lett. 3 (2003) 1049.
[12] S.U.M. Khan, M. Al-Shahry, W.B. Ingler, Science 297 (2002) 2243.
[13] Y. Li, D.S. Hwang, N.H. Lee, S.K. Kim, Chem. Phys. Lett. 404 (2005) 25.
[14] T. Umebayashi, T. Yamaki, S. Yamamot, S. Tanaka, J. Appl. Phys. 93 (2003) 5156.
[15] X. Hong, Z. Wang, W. Cai, F.L. Jun Zhang, Y. Yang, Y. Na Ma, Liu, Chem. Mater. 17 (2005) 1548.
[16] K. Nakumizu, J. Nunoshige, T. Takata, J.N. Kondo, M. Hara, Chem. Lett. 32 (2003) 196.
[17] H. Wang, J.P. Lewis, J. Phys. Condens. Mater. 18 (2006) 421.
[18] T.S. Yang, C.B. Shiu, M.S. Wong, Surf. Sci. 548 (2004) 75.
[19] M.S. Wong, S.B. Chou, T.S. Yang, Thin Solid Films 494 (2006) 244.
[20] S.W. Hsu, T.S. Yang, T.K. Chen, M.S. Wong, Thin Solid Films 515 (2007) 3521.
[21] H. Irie, S. Washizuka, K. Hashimoto, Thin Solid Films 510 (2006) 21.
[22] Y. Li, D.S. Hwang, N.H. Lee, S.J. Kim, Chem. Phys. Lett. 404 (2005) 25.
[23] S. Kelly, F.H. Pollak, M. Tomkiewicz, J. Phys. Chem. B 101 (1997) 2730.
[24] A. Mooradian, P.M. Raccah, Phys. Rev. B 3 (1971) 4253.
[25] R. Wang, N. Sakai, A. Fujishima, T. Watanabe, K. Hashimoto, J. Phys. Chem. B 103 (1999) 2188.